Journal of Structural Engineering Vol.44A(March 1998) JSCE

DYNAMIC CHARACTERISTICS OF ISOLATED BRIDGES CONSIDERING DIFFERENT LOCATION OF SEISIMIC ISOLATION

Jeung-Geun Park*, Hisanori OTSUKA**, Akira KOMIYA*** and Yasuyuki SUZUKI***

*Graduate Student, Dept. of Civil Eng., Kyushu University (6-10-1 Hakozaki, Fukuoka, 812, Japan)
**Dr. of Eng., Professor, Dept. of Civil Eng., Kyushu University (6-10-1 Hakozaki, Fukuoka, 812, Japan)
***Construction Technique Institute Eng. Co., Ltd. (4-9-11 Nihombashi, Honcho, Chuo-Ku, Tokyo, 103, Japan)

The purpose of this paper is to investigate dynamic characteristics of an isolated bridge with a different location of seismic isolation at piers and to determine the best location of seismic isolation. The substructure of the bridge is framed type with double deck and has relatively high piers, so it has long natural period. To decide the best location of seismic isolation, displacement, shear force, bending moment, acceleration and absorbed energy are compared using mode superposition method. To isolate overall structures is effective to bending moments and shear forces for long period bridges.

Key Words : *best location of seismic isolation, long period bridges, bilinear type seismic isolation design*

1. INTRODUCTION

The purpose of this paper is to investigate dynamic characteristics of an isolated bridge with tall flexible piers changing the location of seismic isolation and to determine the best location of seismic isolation.

The selected bridge model has comparatively long natural period, tall piers and heavy superstructure. For restricting moments of piers in this kind of bridge, it is effective to isolate all structure by installing seismic isolation at the bottom of piers or foundations. The representative example is South Rangitikei bridge, New Zealand 1974.[1)]

To express real behaviors of the bridge, the selected bridge is modeled by ADINA(Automatic Dynamic Incremental Nonlinear Analysis) which can analyze a nonlinear three dimensional structure.[3)] Two kinds of elements (beam and truss) are used for representing structural members and isolators. The hysteresis behavior of a selected bridge model is idealized by a bilinear model in the direction of consideration and do not consider geometrical nonlinearities. The earthquake loadings acts to the only one direction (longitudinal direction).

To decide the best location of seismic isolation for the selected model, four isolated bridge models are chosen and displacement, shear force, bending moment, acceleration and absorbed energy are examined under the El Centro NS 1940 which has predominant periods between period 0.4sec and 1.0sec. The design procedure in this paper for each model with bilinear hysteretic isolation is similar to that recommended by Andriono and Carr(1991).[1)]

2. INCREMENTAL EQUATIONS OF EQUILIBRIUM USING MODE SUPERPOSITON

Uncoupling of modal equations is not possible if the system has nonproportional damping or it responds into the nonlinear range. The isolated models in this paper have nonproportional dampings and these equations of motions can be solved by the mode superposition method is proposed by K. J. Bathe[3)] effectively. These techniques have been implemented in ADINA. This procedure is shown as followings.

Using an implicit time integration scheme and the modified Newton iteration to establish dynamic equilibrium at time $t+\Delta t$, the governing finite element equations are

$$M\,{}^{t+\Delta t}\ddot{U}^{(i)}+C\,{}^{t+\Delta t}\dot{U}^{(i)}+{}^{0}K\cdot\Delta U^{(i)}={}^{t+\Delta t}R-{}^{t+\Delta t}F^{(i-1)} \quad (1)$$

where

$${}^{t+\Delta t}U^{(i)}={}^{t+\Delta t}U^{(i-1)}+\Delta U^{(i)} \quad (2)$$

i is iteration, M is constant mass matrix, ${}^{t+\Delta t}\ddot{U}^{(i)}$ is acceleration, C is constant damping matrix, ${}^{t+\Delta t}\dot{U}^{(i)}$ is velocity, ${}^{0}K$ is stiffness matrix corresponding to the configuration and material properties at time 0, $\Delta U^{(i)}$ is displacement increment, ${}^{t+\Delta t}R$ is external point load vector due to body forces, surface loads and concentrated loads, ${}^{t+\Delta t}F^{(i-1)}$ is nodal point force vector equivalent to the element stresses that correspond to displacements, ${}^{t+\Delta t}U^{(i-1)}$.

Using Eq.(1), a constant effective stiffness matrix is formed in the time integration, and thus only one triangular matrix factorization is needed in the calculation of the dynamic response. All nonlinearities are taken fully into account in the evaluation of the vector ${}^{t+\Delta t}F^{(i-1)}$.

In this transformation we use

$$ {}^{t+\Delta t}U \cong \Phi \cdot {}^{t+\Delta t}X \qquad (3) $$

where

$$ {}^{t+\Delta t}X = \begin{bmatrix} {}^{t+\Delta t}x_1 \\ \cdot \\ \cdot \\ {}^{t+\Delta t}x_p \end{bmatrix}, \quad \Phi = \left[\phi_1, \ldots, \phi_p\right] \qquad (4) $$

The values ${}^{t+\Delta t}X$ are the generalized modal displacements at time $t+\Delta t$ and the vectors Φ are the eigenvectors of the generalized eigenproblem,

$$ {}^{0}K \cdot \phi_i = \omega_i^2 \cdot M \cdot \phi_i \qquad (5) $$

where the ω_i are the natural circular frequencies of the linearized system at time 0.

Substituting from Eq.(3) into Eq.(1), we obtain

$$ \begin{aligned} &{}^{t+\Delta t}\ddot{X}^{(i)} + \Lambda \cdot {}^{t+\Delta t}\dot{X}^{(i)} + \Omega^2 \cdot \Delta X^{(i)} \\ &= \Phi^T \left({}^{t+\Delta t}R - {}^{t+\Delta t}F^{(i-1)} \right) / M \end{aligned} \qquad (6) $$

$$ \Lambda = \begin{bmatrix} 2\xi_1\omega_1 & & \\ & \cdot & \\ & & \cdot \\ & & & 2\xi_p\omega_p \end{bmatrix}, \quad \Omega^2 = \begin{bmatrix} \omega_1^2 & & \\ & \cdot & \\ & & \cdot \\ & & & \omega_p^2 \end{bmatrix} \qquad (7) $$

where the Λ are diagonal matrix listing proportional dampings, the Ω^2 are diagonal matrix listing circular frequencies, the ξ are the modal damping ratios corresponding to the ω and p is the number of degree of freedom in modal.

It should be noted that, different from linear analysis, the incremental equilibrium equations in the new basis, Eq.(6) are still coupled, because the nodal point force vector, ${}^{t+\Delta t}F^{(i-1)}$ can only be evaluated once all displacements are known,

$$ {}^{t+\Delta t}U^{(i-1)} = \sum_{k=1}^{p} \phi_k \cdot {}^{t+\Delta t}x_k^{(i-1)} \qquad (8) $$

Since Λ and Ω^2 are diagonal matrices and only p equations are considered, the solution of the eigenproblem in Eq.(5) plus the step-by-step solution of Eq.(6)(using the Newmark method) can be significantly more cost-effective than the direct step-by-step solution of Eq.(1).

3. STRUCTURAL MODEL FOR EVALUATION

Fig.1 shows 3D(Three Dimension) FEM(Finite Element Method) modeling for the selected bridge. Superstructure has two stories steel box girders with 11.15m width and substructure consisting of twelve piers with 22.7m high. The total weight of bridge is about 16,574tf. The ratio of mass distributions is 0.48 at the upper girder, 0.48 at the lower girder and 0.04 at the pier. These facts show that the large amount of mass are concentrated on superstructure. The selected ordinary bridge has comparatively long the first natural period of 0.97sec also. This kind of bridges is unstable for an overturning in the transverse direction and must be prepared for overturning. Characters 'C' and 'B' mean column and beam of piers and characters from 'P1' to 'P12' sign piers. The total number of nodes is 364 and the total number of elements (3D beam elements(240) and truss elements(72)) is 312. Here, the 3D beam elements are used for girders and piers and the truss elements are used for horizontal stiffness and vertical stiffness of isolators. Girders and piers are modeled as linear elastic 3D beam element and can have any arbitrary cross-sectional geometry. The longitudinal direction stiffness K_{bl} and transverse direction stiffness K_{bt} of isolators are modeled as bilinear material model having kinematic strain hardening. The yield stress is assumed to be the same in tension and compression. Vertical stiffness K_v is modeled as linear elastic. For simplicity, the same stiffness for the K_{bl} and K_{bt} are used and the vertical stiffness K_v is considered as about 20times of horizontal stiffness. For connecting girders and piers, Rigid Link is used. The Rigid Link is a special constraint equation established between two nodes – the master node and slave node in ADINA.

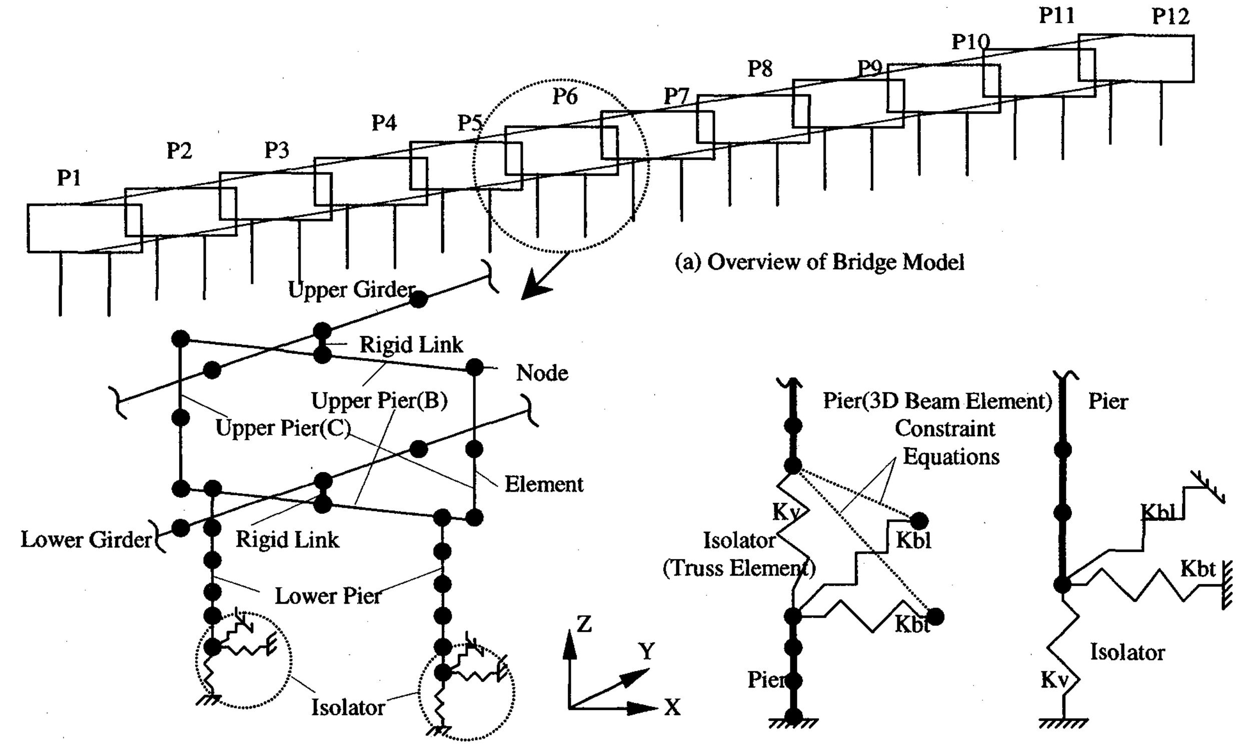

(a) Overview of Bridge Model

(b) Node and Element

(c) Modeling of Isolator for Two Cases

Fig.1 3D FEM Modeling for a Selected Bridge

Table 1 Properties of Members

Structural Member	$I_r(m^4)$	$I_s(m^4)$	$I_t(m^4)$	$A(m^2)$	W(tf/m)
Upper Girder	0.80	0.80	0.40	0.30	8.2
Lower Girder	0.80	0.80	0.40	0.30	8.2
Upper Pier(C)	0.13	0.12	0.12	0.12	1.8
Upper Pier(B)	0.18	0.16	0.16	0.16	1.8
Lower Pier	0.26	0.13	0.13	0.17	1.8
Foundation	0.70	0.60	0.30	0.49	1.8

As the nodes displace due to deformation, the slave node is constrained to translate and rotate. Large displacements and rotations can be considered, using the Updated Lagrangian formulation for the isolated structure also.[2)]

Table 1 shows properties of structural members. I_r, I_s and I_t are the second moment of area with respect to local coordinate r, s and t. The r, s and t are corresponded to global coordinate X, Y and Z respectively. A is area of member section and W is weight per unit length.

To investigate the behaviors of bridges due to different location of isolator, four isolated bridge models are selected as shown in Fig.2. These isolators are installed at different location of piers excepting Isolated D. In case of Isolated D, the isolator is installed between foundations.

In this paper, the vertical stiffness is considered as liner since the earthquake loadings is acted to the longitudinal direction only but if earthquake loadings are acted to the two or more directions, large rotations will be occurred to the transverse direction. In this case, the nonlinear behavior of vertical stiffness of isolator must be considered. Furthermore, a bridge having a heavy superstructure must be prepared against an overturning for the transverse direction.

The optimum yield ratio Q_y/W for minimum base shear in earthquake motions corresponding approximately to the El Centro accelerogram is around 0.04 ~ 0.05, for T_{b2}=1.5~2sec[1)]. In this paper, the value of Q_y/W of 0.05 is used. Eq.(9) shows the composite horizontal stiffness for considering pier bending stiffness.

$$K_b' = \frac{K_b}{1+\frac{K_b}{K_p}} \qquad (9)$$

Where K_b' is composite stiffness considering flexibility of piers, K_b is horizontal stiffness of isolator and K_p is bending stiffness of piers. Generally, the weight of piers can be disregarded in computing an earthquake response because its weight is very small comparing superstructures and do not have influence on the 1st mode. In this paper, by FEM modeling the flexibility and the weight of piers are considered. Even if the stiffness of piers is used, the yielding force of device Q_y does not change for each model.

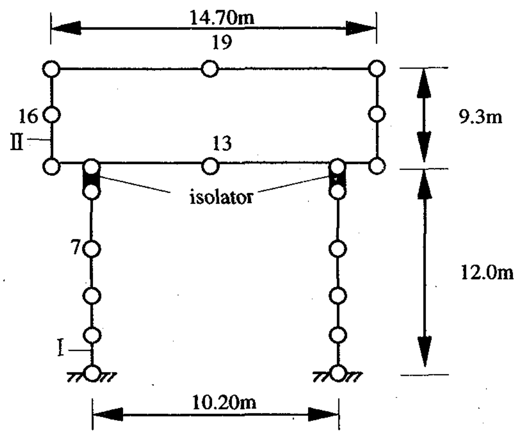

(a) Isolated A

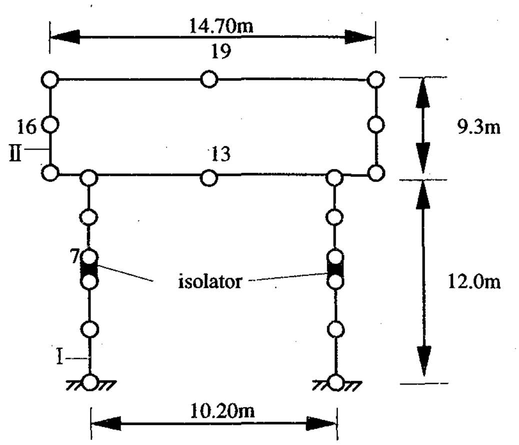

(b) Isolated B

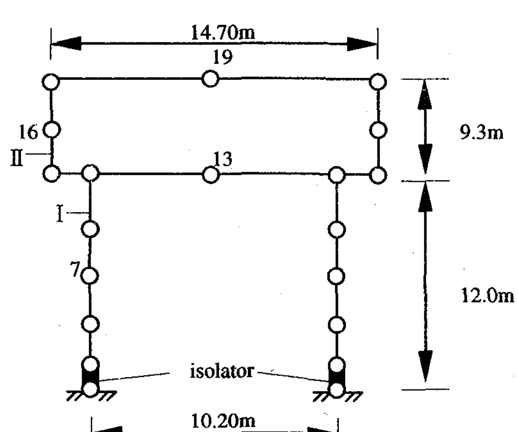

(c) Isolated C

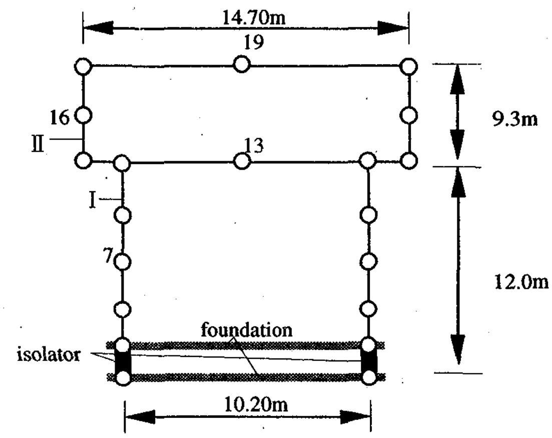

(d) Isolated D

Fig.2 Models with Different Installation of Seismic Isolation

4. SEISMIC ISOLATION DESIGN FOR BILINEAR TYPE DEVICE

Design Concept

In principle, design earthquakes for seismically isolated structures should be selected on the same general basis as design earthquakes for a conventional structure. In this paper, the conventional acceleration response spectra is used for designing the isolated structures.

The El Centro NS 1940 seismic loadings include predominant periods from 0.4sec to 1.0 sec. In these periods, especially large displacements occur between 0.5 sec and 0.6 sec. Because a resonance is occurred in these periods. Seismic isolation structures can decrease accelerations as escaping the resonance by increasing natural period. Therefore, periods range from 1.5 sec to 3.0 sec can be selected as a target period. Here, we choose the first natural periods range from 1.6 sec to 2.3 sec for the isolated models.

Design Procedure

A design procedure can be classified into two stages largely. The first stage is preliminary design, the second stage is detailed design. At the preliminary design stage, we determine structural form, isolator parameter and tentative assignment of member sizes etc.. In detailed design stage, optimization of the aseismic design and more detailed design of the structure and isolator are conducted. In this stage, we must examine more accurate evaluations of seismic response using dynamic analysis also.

Often design motions are specified in terms of 5% damped acceleration response spectra. In this paper, we choose El Centro earthquake loadings having maximum acceleration of 320 cm/sec^2 as the design level. The acceleration response spectra may be converted to the required displacement form which expressed as $S_D(T,\xi)$ by using Eq. (10).[1)]

$$S_D(T,\xi)=\frac{0.39gTC_D(\xi)}{4\pi^2}=9.7TC_D(\xi)\ \text{(cm)} \quad (10)$$

where S_D is converted displacement response spectrum, g is gravity acceleration, T is period of structure, ξ is damping ratio and C_D is damping-dependent coefficient.

Fig.3 shows the relation between force and displacement for the isolator. T_{b1} of 1.2sec and T_{b2} of 3.0sec are used for all isolated models in this paper. Where S_b is maximum shear force of isolator, X_b is maximum relative displacement of isolator, Q_y is yielding force of isolator, Q_d is force for damper, X_y is yielding displacement and T_{b1} is period associated with elastic stiffness K_{b1} and T_{b2} is period associated with plastic stiffness K_{b2}.

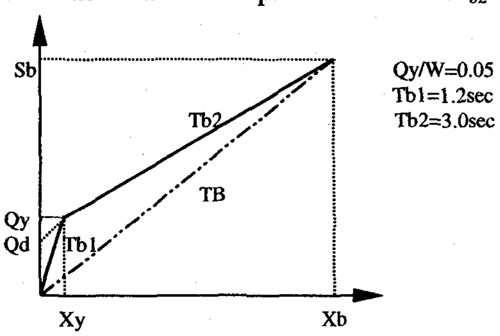

Fig.3 Force and Displacement for Isolator

The yield-force ratio Q_y/W of the combined rubber-bearing and steel-beam isolation system is given by Eq.(11) from Fig.3

$$\frac{Q_y}{W}=\frac{T_{b2}^2}{T_{b2}^2-T_{b1}^2}\frac{Q_d}{W} \quad (11)$$

where W is total weight of superstructure. From the relationship of Eq.(11), we can choose isolator parameter Q_y/W, T_{b1} and T_{b2} tentatively.

The estimation of the seismic response for a structure with bilinear hysteretic isolation can be accomplished by iterative calculation using Eq.(12), (13) and (14).[1)]

$$\frac{S_b}{W}=\frac{Q_y}{W}\left(1-\frac{T_{b1}^2}{T_{b2}^2}\right)+\frac{4\pi^2X_b}{gT_{b2}^2} \quad (12)$$

$$T_B=2\pi\sqrt{\frac{X_b}{\left(\frac{S_b}{W}\right)g}} \quad \text{(sec)} \quad (13)$$

$$\xi_B=\frac{2}{\pi}\frac{(Q_y/W)}{(S_b/W)}\left(1-\frac{T_{b1}^2}{T_B^2}\right) \quad (\%) \quad (14)$$

where T_B is effective period for bilinear isolator and ξ_B is effective damping ratio of bilinear isolator. By response spectra, the maximum displacement, acceleration and seismic force can be obtained under the El Centro type earthquake loadings. The isolator of these bridge models have high non-linearity (about 61%) which can be calculated the formula defined by R.I. Skinner[1)] and high plastic flexibility for decreasing shear force effectively. The major advantage of this type is very low base shears and insensitive to strength of seismic load. The responses of structures are influenced by distribution of masses, mechanical characteristics of device and high mode vibration etc.

Table 2 shows an example for the estimation of design displacement by Eq.(10), (12), (13) and (14). At first, maximum displacement of isolator is assumed and the design displacement of the selected model using response spectra is obtained by iteration as 8.15cm at the 2nd step for Isolated A.

Table 2 Estimation of Design Displacement

	1st step	*2nd step*
X_b(cm)	*12.00*	*8.00*
S_b/W	*0.092*	*0.060*
T_B(sec)	*2.84*	*2.47*
ζ_B	*0.44*	*0.46*
$C_D(\zeta_B)$	*0.37*	*0.34*
$S_D(T_B, \zeta_B)$(cm)	*10.19*	*8.15*

Design Result

Table 3 shows the seismic isolation design results according to different location of seismic isolation.

Table 3 Design Result (unit : kgf, cm, sec)

	Isolated A	*Isolated B*	*Isolated C*	*Isolated D*
W	*555700*	*567760*	*579820*	*585630*
Q_y	*27785*	*28388*	*28991*	*29282*
T_{b1}	*1.2*	*1.2*	*1.2*	*1.2*
T_{b2}	*3.0*	*3.0*	*3.0*	*3.0*
K_{b1}	*15545*	*15874*	*16230*	*16395*
K_{b2}	*2487*	*2540*	*2597*	*2623*
S_b	*33342*	*34066*	*34789*	*35138*
**E_{b1}*	*15545*	*15874*	*16230*	*16395*
**E_{b2}*	*2487*	*2540*	*2597*	*2623*
**σ_y*	*2779*	*2839*	*2899*	*2928*

In Table 3, E_{b1} is elastic modulus corresponding

K_{b1}, E_{b2} is strain hardening corresponding K_{b2} and σ_y is yielding stress of isolator. These $^*E_{b1}$, $^*E_{b2}$ and $^*\sigma_y$ will be used in the program ADINA.

5. BEHAVIORS OF ISOLATED BRIDGE MODELS

Several mechanical characteristics, bending moment, shear force, displacement, acceleration and absorbed energy are examined to determine the best location of seismic isolation for the longitudinal direction. Table 4 shows the analysis results at P6 for the selected models including the ordinary bridge by absolute maximum values. Where 'location' means measuring points of each model in Fig.2. T_1 is the first natural period of models.

The first natural periods of models are changed due to stiffness of piers even if each isolator is designed by similar values as shown in Table 3. Especially Isolated C and D have more flexible Lower Pier than Isolated A and B, thus the periods of Isolated C and D become lengthened.

Table 4 Analysis Results (absolute maximum value for longitudinal direction at P6)

Item	*Ordinary*	*Isolated A*	*Isolated B*	*Isolated C*	*Isolated D*	*location*
Displacement u_{max} *(cm)*	*3.82*	*1.05*	*6.06*	*13.94*	*14.23*	*7*
	11.39	*10.46*	*9.03*	*20.03*	*20.37*	*13*
	16.87	*11.54*	*10.84*	*23.22*	*23.59*	*16*
	25.66	*12.86*	*12.66*	*26.18*	*26.57*	*19*
Acceleration a_{max} *(cm/sec²)*	*203.13*	*50.51*	*273.11*	*266.74*	*274.41*	*7*
	606.37	*504.74*	*407.26*	*383.33*	*393.32*	*13*
	967.64	*556.84*	*488.86*	*444.45*	*454.93*	*16*
	1366.52	*620.58*	*571.04*	*500.9*	*512.95*	*19*
Shear Force F_{max} *(kgf)*	*4.56E5*	*1.11E5*	*9.04E4*	*1.09E5*	*1.10E5*	*I*
	3.17E5	*6.30E4*	*5.4E4*	*6.32E4*	*6.38E4*	*II*
Moment M_{max} *(kgf-cm)*	*5.30E8*	*1.48E8*	*6.00E7*	*1.07E5*	*1.08E5*	*I*
	1.07E8	*2.61E7*	*2.64E7*	*2.15E7*	*2.16E7*	*II*
T_1*(sec)*	*0.973*	*1.604*	*1.665*	*2.230*	*2.238*	.

Validation:

The degree of estimation of responses by the seismic isolation design method used in this paper can be validated by comparing the time history analysis for 3D FEM model. Here, for Isolated A, a longitudinal displacement at P6 is compared. There is 13% difference between the design result in Table 2 and the time history analysis result in Table 4 as shown in (15). This difference may be acceptable and the design method used in this paper can thus be used with confidence in selecting design parameter for preliminary and conceptual design.

$$S_D(T_B, \xi_B) = 8.15cm \cong u_{\max,I} = 7.1cm \qquad (15)$$

Displacement and Structural Deformation:

Fig.4 (a), (b) and (c) show the relative displacements of upper girder, isolator and relative displacement of structure respectively. Where O, A, B, C and D mean Ordinary bridge, Isolated A, Isolated B, Isolated C and Isolated D respectively. In Fig.4 (a), the ordinary bridge has large displacement since the ordinary bridge has long first natural period (0.97sec) and long piers comparatively. Among isolated models, Isolated C and Isolated D have large displacement because the continuous length of pier is longer than Isolated A and Isolated B.

In Fig.4 (b), the displacements on isolators are the similar values among Isolated models since the weight at the upper part of isolator is similar.

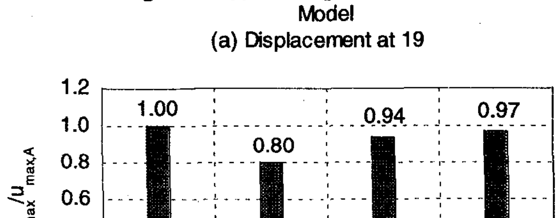

(a) Displacement at 19

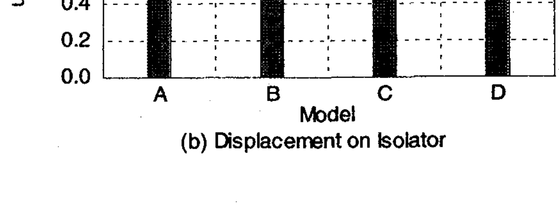

(b) Displacement on Isolator

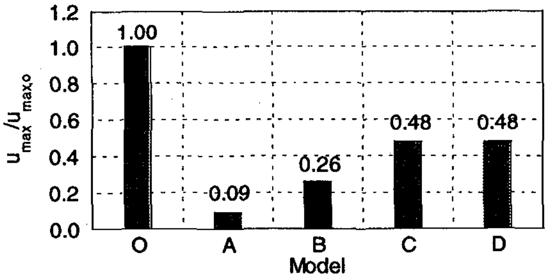

(c) Relative Displacement

Fig.4 Displacement and Structural Deformation

Fig.4 (c) shows the relative displacement between node 19 and top of isolators. The relative displacement of isolated models are very small comparing the ordinary bridge. This fact shows that the isolated structure is more effective than ordinary structures for internal forces, shear forces and bending moments etc.

Acceleration :

Fig.5 (a) and (b) show accelerations at girders and at the center of piers. The acceleration is related to the serviceability of secondary structures, for example, water pipe etc. In Fig.5 (a), the acceleration of isolated models are smaller than that of the ordinary bridge.

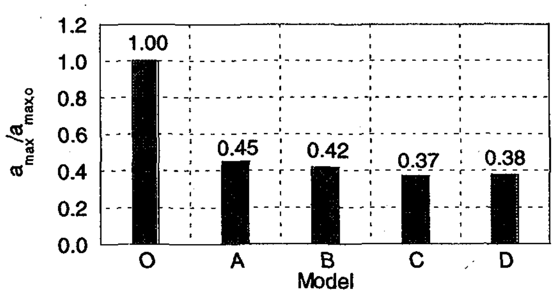

(a) Acceleration at 19

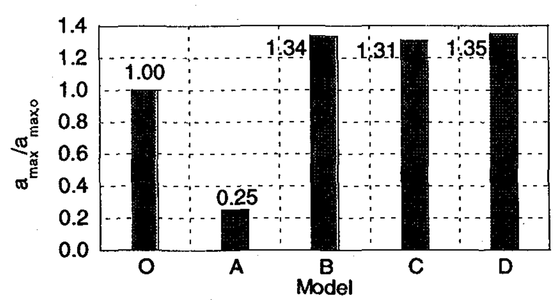

(b) Acceleration at 7

Fig.5 Acceleration

Generally, the acceleration at girder is decreasing by about two times of that of the ordinary bridge regardless location of seismic isolation and mass of foundation. But at piers as shown in Fig.5 (b), accelerations are increased largely. This fact may be explained by a higher mode effects. Commonly, a flexible part or a secondary structure of structures are affected by the higher modes and accelerations may be increased.

Isolated A has very small relative acceleration at center of piers. Because the relative acceleration(with respect to ground) of the upper part of isolator is larger than that of the lower part of isolator according as the inertial forces are not transferred in the condition of an equivalent fixed-base system.

Shear Force and Bending Moment:

Fig.6 (a), (b), (c) and (d) show lateral forces and bending moments each measuring points of P6.

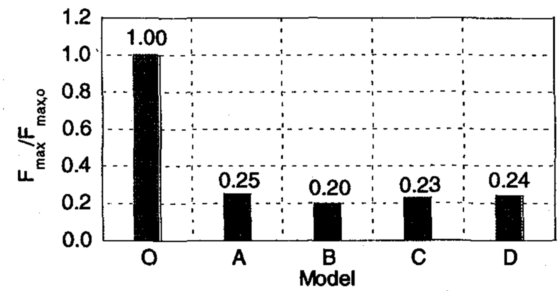

(a) Shear Force at I

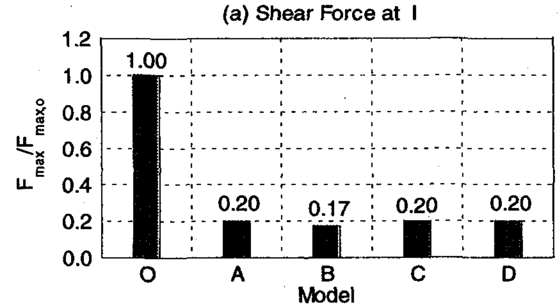

(b) Shear Force at II

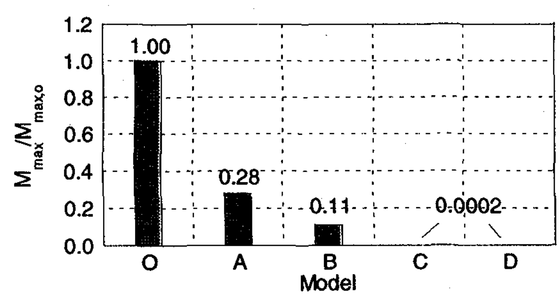

(c) Bending Moment at I

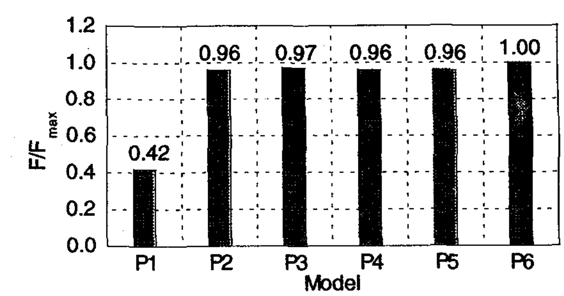

(d) Shear Force at Piers

Fig.6 Shear Force and Bending Moment

Shear forces are decreased remarkably under earthquake loadings regardless the location of seismic isolation as shown in Fig.6 (a) and (b).

In case that a bridge has comparatively long period, the bending moment can be decreased largely by isolating overall structures as shown in Fig.6 (c).

Fig.6 (d) shows the shear force at piers for the ordinary bridge. Here, the pier P1 located at the end of the bridges has shear forces less than about two times that of others. This fact shows that the isolator of P1 undertake smaller shear forces than others.

Absorbed Energy:

Commonly, an earthquake total input energy can be absorbed by viscous damping or plastic deformation. As for LRB (Lead Rubber Bearing), the lead can be absorbed mainly by hysteretic deformation and can evaluate an earthquake resistance using a hysteretic absorbed energy E_h as comparing a total input energy. By Eq.(16), the hysteretic absorbed energy can be calculated.

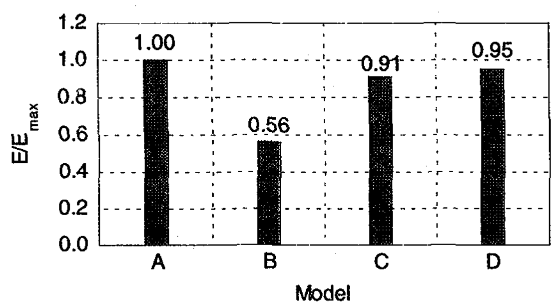

Fig.7 Absorbed Energy

Excepting Isolated B, other isolated models have similar ability of absorbing energy. Here, we can see that installing seismic isolation at center of pier is not good for the absorbing energy and the maximum relative deformation of isolator $u_{max,I}$ increases as the absorbed energy increases as shown in Table 5.

The (17) means that an absolute accumulated ductility ratio μ_c defined as (18) on an isolator at P6 which has a maximum value between the plus accumulated ductility ratio μ_c^+ and the minus accumulated ductility ratio μ_c^-. The designed isolator has high accumulated ductility ratio average 225.91. This means the isolator has very high plastic phase, so can decrease lateral force at base and insensitive to strength of seismic load.

$$E_h = {}^tK \int_{t_s}^{t_e} u\dot{u}dt \cong \sum F_i \Delta u_i \qquad (16)$$

$$\mu_c = Max\left(\mu_c^+, \mu_c^-\right) \qquad (17)$$

$$\mu_c^+ = 1 + \frac{\delta_p^+}{\delta_e}, \mu_c^- = 1 + \frac{\delta_p^-}{\delta_e} \qquad (18)$$

where ${}^tK$ is stiffness changing by time t, t_s is earthquake starting time, t_e is earthquake ending time, u is relative displacement of isolator, $\dot{u}$ is velocity corresponding u, F_i are inertial force due to earthquake loadings, Δu_i are displacement increment at i, δ_p^+ is plus accumulated plastic deformation, δ_p^- is minus accumulated plastic deformation and δ_e is yield deformation.

Table 5 Absorbed Energy , Accumulated Ductility Ratio and Maximum Displacement

	Isolated A	*Isolated B*	*Isolated C*	*Isolated D*
E_h*(kgf-cm)*	*1.80E6*	*1.04E6*	*1.63E6*	*1.73E6*
$\mid \mu_c \mid$	*237.28*	*161.27*	*246.24*	*258.83*
$\mid u_{max,I} \mid$ *(cm)*	*7.1*	*5.7*	*6.7*	*6.9*

Best Location of Isolation

Table 6 shows decision-making table for selecting best location of isolator. Here, we choose five items, Cost & Maintenance, Absorbed Energy, Shear Force, Moment and Acceleration in order of priority for determining the best location of seismic isolation.

The cost and maintenance are most important factor to evaluate the feasibility of adopting seismic isolation. By adopting seismic isolation, we can economize costs as about 5%.[1] The second important item for evaluating is absorbed energy. The degree of absorbing energy of structural member against external earthquake loadings is corresponding to the earthquake resistance. Next, the shear force and moment are main mechanical characteristics to control the section of piers and the accelerations are corresponded to the serviceability of secondary structures through the bridge.

For evaluation, we give values to importance factor IF according to order of priority as shown in Table 6. Each model is graded by No Good, Good and Excellent with respect to IF. The score is calculated by the following calculation (19) from the analysis results in Table 4.

$$Score = \sum Grade \times IF \qquad (19)$$

where we define the Grade are No Good = 0.4, Good = 0.7 and Excellent = 1.0. Here, the values of IF and Grade are just defined values to show differences of Score calculated according to importance.

In Table 6, the Isolated C which is adopted overall isolation can be recommended as the appropriate location of seismic isolation for the bridges having long period. Isolated D is not good for the cost and maintenance because the device is installed between foundations below ground level. The shear forces are decreased effectively all isolated models comparing the ordinary model. Isolated B is not good for the absorbed energy among isolated models. The accelerations at upper girder are decreasing for all isolated models comparing the ordinary model. From these results, the Isolated C is good for all items selected.

Table 6 Decision-Making Table for Selecting Best Location

Item(IF)	*Isolated A*	*Isolated B*	*Isolated C*	*Isolated D*
Cost & Maintenance(1.0)	*Good*	*Good*	*Good*	*No Good*
Absorbed Energy(0.9)	*Excellent*	*No Good*	*Excellent*	*Excellent*
Shear Force(0.8)	*Excellent*	*Excellent*	*Excellent*	*Excellent*
Bending Moment(0.7)	*Good*	*Good*	*Excellent*	*Excellent*
Acceleration(0.6)	*Good*	*Good*	*Good*	*Good*
Score	*3.31*	*2.77*	*3.52*	*3.22*
Rank	*2*	*4*	*1*	*3*

6. CONCLUSIONS

1) To isolate overall structures is an effective method to decrease bending moments for long period bridges with tall piers as shown in Isolated C and D.
2) Accelerations is decreased at girders as much as half of that of the ordinary bridge but is increased largely at piers for the isolated bridge models.
3) Shear forces and bending moments at piers are decreased remarkably regardless the location of seismic isolation.

REFERENCES

1) R. I. Skinner, W. H. Robinson and G. H. McVerry : *An Introduction to Seismic Isolation,* John Wiley & Sons Ltd. , U.S.A, 1996.
2) K. J. Bathe : Automatic Dynamic Incremental Nonlinear Analysis, ADINA engineering, U.S.A., 1984.
3) K. J. Bathe and Sheryl Gracewski : On nonlinear dynamic analysis using substructuring and mode superposition, *Computers & Structures,* Elsevier Science, Great Britain, 1981.

(Received September 26, 1997)